# Rate dependence of serrated flow during nanoindentation of a bulk metallic glass

C.A. Schuh and T.G. Nieh
*Materials Science and Technology Division, Lawrence Livermore National Laboratory, Livermore, California 94550*

Y. Kawamura
*Department of Mechanical Engineering and Materials Science, Faculty of Engineering, Kumamoto University, Kumamoto, 860, Japan*

(Received 8 January 2002; accepted 8 April 2002)

Plastic deformation of Pd–40Ni–20P bulk metallic glass (BMG) was investigated by instrumented nanoindentation experiments over a broad range of indentation strain rates. At low rates, the load–displacement curves during indentation exhibited numerous serrations or pop-ins, but these serrations became less prominent as the indentation rate was increased. Using the tip velocity during pop-in as a gauge of serration activity, we found that serrated flow is only significant at indentation strain rates below about 1–10/s. This result suggests a transition in plastic flow behavior at high strain rates, in agreement with prior studies of BMGs under different modes of loading.

## I. INTRODUCTION

Although bulk metallic glasses (BMGs) exhibit desirable room-temperature strength, typically near 2 GPa, plastic strain in these materials is carried by narrow bands of shear localization. In tension, this shear banding leads to low ductility and rapid shear-off failure along a single plane inclined to the stress axis.[1] In other modes of loading, shear bands appear to nucleate and propagate in discrete bursts, giving rise to rapid plastic strain development at a critical stress level. For example, after the yield stress has been reached during quasi-static compression of Pd- or Zr-based BMGs, serrated plastic flow is observed, where the stress-strain curve is not smooth, but punctuated by many small load drops.[2–6] These serrations have been correlated with the motion of individual shear bands through the specimen, where each contributes a small increment of plastic strain to the macroscopic stress–strain curve.[2] The importance of shear bands in plastic deformation of BMGs is emphasized by recent results on BMG composite materials, where the interception of shear bands by a dispersed second phase impacts the global deformation response and can substantially increase tensile ductility.[7–9]

Although serrated flow of BMGs is most commonly observed under uniaxial compression,[2–6] it has also been observed under more complex stress states. For example, Kimura and Masumoto[10,11] have measured displacement bursts during mode-I crack opening experiments on a Pd–6Cu–16Si amorphous metal, and observed the development of shear bands on the exposed surfaces of specimens during testing. In a separate work, these authors found similar results during a mode-III tear test of thin amorphous metallic ribbons.[12,13] Kimura and Masumoto[4,10–13] also demonstrated that plastic deformation by shear band propagation follows an Arrhenius-type kinetics and that flow serrations disappear at high rates of displacement. This suggests that shear band nucleation/propagation is a rate-dependent process.

Recent investigations by Wright *et al.*[2] and Golovin *et al.*[14] have pointed out that nanoindentation may be used to probe details of serrated flow behavior in BMGs. Working with a Zr-based BMG, Wright *et al.*[2] observed the onset of plastic flow during nanoindentation as a discontinuity in the load–displacement curve, and attributed this "pop-in" to the nucleation of a shear band beneath the indenter tip. Aside from this isolated pop-in, there was no other clear evidence of shear-band activity in the load–displacement curve, a result consistent with the recent study by Vaidyanathan *et al.,*[15] who measured a smooth load–displacement curve to depths as large as 10 μm on a similar alloy. Although Vaidyanathan *et al.*[15] did not study pop-in events, they did observe shear bands *ex situ,* both in and around their Berkovich indentations. In contrast with these studies on Zr-based BMGs, the nanoindentation results of Golovin *et al.*[14] exhibit pronounced serrations in the load–displacement curves of a Pd–30Cu–10Ni–20P alloy, not only at the initial onset of plastic deformation (as in the work of Wright *et al.*[2]) but at multiple loads during a single test. In this article, we extend the use of nanoindentation for the study of serrated flow, by examining the influence of indentation strain rate in a Pd-based BMG.

  

## II. EXPERIMENTAL

The BMG used in this work was of composition Pd–40Ni–20P (at.%), prepared by heating pure Pd, Ni, and P up to 1127 K at a slow heating rate of 1 K/min. The ingot was melted with $B_2O_3$ in an evacuated quartz tube with an inner diameter of 5 mm and followed by water quenching; details of the processing and verification of the amorphous nature of the alloy are available in Refs. 1 and 16. The specimen was mechanically polished to a mirror finish and tested in a TriboIndenter instrumented nanoindenter (from Hysitron, Minneapolis, MN), using constant loading rates from $8 \times 10^{-5}$ to $2 \times 10^{-2}$ N/s, with peak applied loads of 10 mN. In all of the experiments, a spherical diamond indenter with a radius of 450 nm was used and care was taken to ensure that the thermal drift of the instrument was maintained below 0.5 nm/s. Data were acquired at sampling rates as high as 6000 Hz, to measure the velocity of rapid pop-in events.

## III. RESULTS AND DISCUSSION

The loading portions of the load–displacement ($P$–$h$) curves are shown for typical indentations in Fig. 1, for four different loading rates spanning the range $6 \times 10^{-4}$–$2 \times 10^{-2}$ N/s. For the indentations performed at lower loading rates, these curves are punctuated by discontinuities, or "pop-ins", in which the displacement increases at an approximately constant load. For continuum plastic yielding such pop-ins are not expected, and in crystalline materials their presence is invariably associated with discrete plastic deformation phenomena, such as cracking or dislocation nucleation.[17–21] In BMGs, these discontinuities are likened to the serrated flow observed in other modes of loading and are associated with the nucleation and motion of shear-bands.[2,14] As observed in Fig. 1, the character of the pop-ins in Pd–40Ni–20P depends on the rate of loading; slow loading conditions appear to promote pop-ins over a broader range of loads and lead to sharper, more horizontal discontinuities. At higher loading rates, the pop-ins appear less as horizontal bursts than as gentle ripples in the load–displacement curve, each one extended over a range of loads. Also, the depth of individual pop-ins increases with increasing load or depth, suggesting that the shear displacement of individual shear bands increases with the size scale of the indentation. Finally, although changes in the indentation rate cause changes in the serrated plastic flow of the BMG, the global shape of the curves in Fig. 1 is very similar at all rates. This result suggests that the hardness or yield strength of this alloy is only weakly dependent on loading rate, as also observed in the work of Mukai *et al.*[1] on the same alloy under tensile loading.

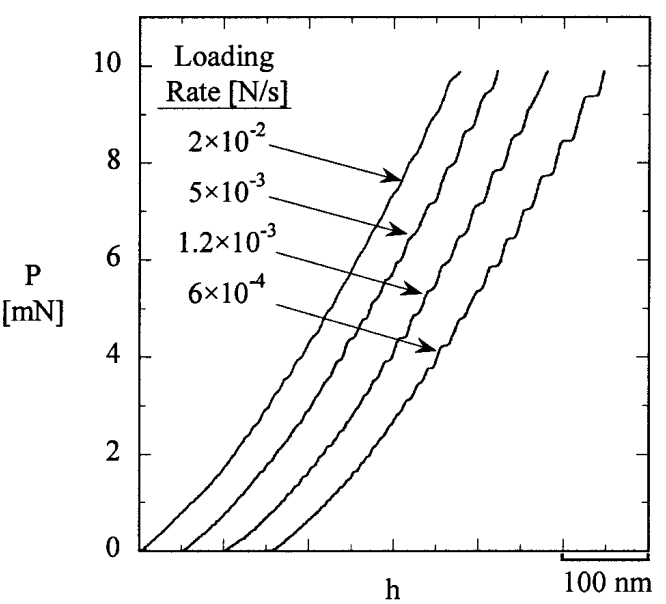


FIG. 1. Load ($P$) plotted against indentation depth ($h$) for the loading segment of four indents on Pd–40Ni–20P with different loading rates.

The indentation strain rate is defined as $\dot{\epsilon} = (1/h)\, dh/dt$ and is a function of time during a constant loading-rate indentation experiment. In Fig. 2, the indentation strain rate is plotted for three indentations with different loading rates, as a function of the indentation depth. At the outset of the indentation ($h \sim 0$), the strain rate is very high and diminishes with the quantity $1/h$ as the indentation proceeds. As shown in Fig. 2, the nanoindentation method is capable of sampling a broad range of indentation strain rates, from low rates below $10^{-2}$/s to those as high as 10–100/s. Although the strain rate decreases throughout the test history, the trend is not smooth but is punctuated by many short bursts to higher strain rates. These peaks are small for the specimens indented at high loading and/or strain rates and became more pronounced as the loading or strain rate is decreased. Each peak represents a short period during which the indenter tip sinks quickly into the specimen, i.e., a pop-in event. Peaks such as those shown in Fig. 2 can be exactly correlated to the pop-in discontinuities observed in the load–displacement curves (Fig. 1).

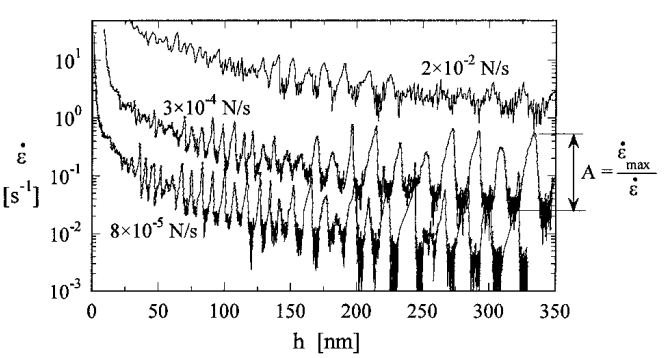


FIG. 2. Indentation strain rate as a function of the indenter penetration depth upon loading. The general decrease in strain rate is punctuated by rapid bursts during pop-in events.

In both Figs. 1 and 2, a clear trend is observed where pop-in events, or serrations, become more prominent with lower loading or indentation strain rates. This trend is quantified by considering the normalized height, $A = \dot{\epsilon}_{max}/\dot{\epsilon}$, of the strain-rate peaks in Fig. 2. As illustrated for a single peak in Fig. 2, $\dot{\epsilon}_{max}$ is the maximum strain rate measured at the tip of the peak, and $\dot{\epsilon}$ is the average "background" strain rate surrounding the peak. The normalized height A thus represents the factor by which deformation is accelerated during a pop-in event. In Fig. 3, the influence of the applied strain rate on A is shown, sampling from many indentations at various loading rates. Because of the noise in the curves of Fig. 2, the data points in Fig. 3 have been assigned large error bars of ±50% in $\dot{\epsilon}$.

Although the scatter in the data is significant, Fig. 3 quantifies the trends observed earlier in Figs. 1 and 2, illustrating a decrease in the prominence of flow serration as the indentation strain rate increases. At a critical indentation strain rate in the range 1–10/s, the normalized peak height approaches the limiting value of unity, where there are no pop-in events at all. It is important to note that although the indentation strain rate is qualitatively useful, it quantitatively overestimates the true rate of strain development in the material[22,23] and is related to an equivalent, uniaxial strain rate, $\dot{\epsilon}_u = C\dot{\epsilon}$, where the constant $C \approx 0.1$ has been found for amorphous selenium in Ref. 22. Therefore, the equivalent strain rate at which the serrations vanish is probably in the range $\dot{\epsilon}_u = 10^{-1}$–1/s; this scale is also illustrated on the upper axis of Fig. 3.

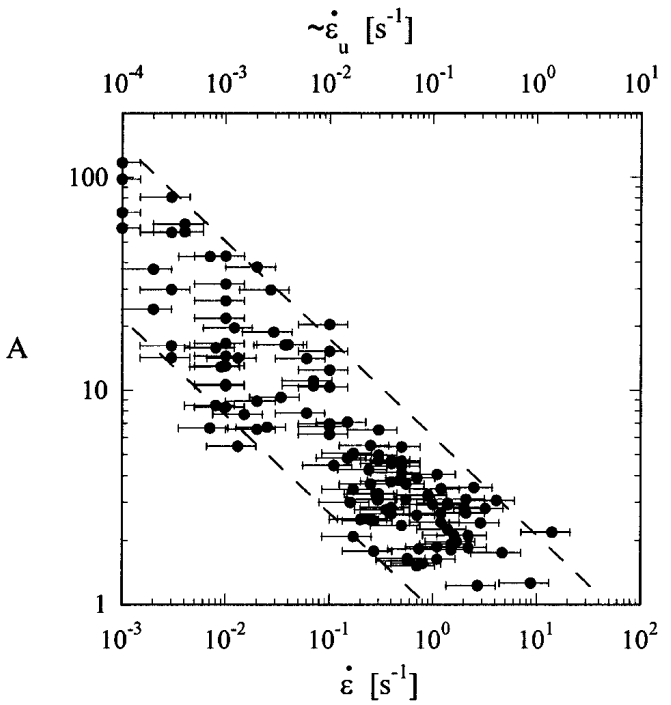


FIG. 3. Indentation strain rate dependence of the pop-in velocity. The quantity A defined in Fig. 2 represents the factor by which deformation accelerates during a pop-in. An approximate scale for the equivalent uniaxial strain rate is also presented for comparison.

The data in Fig. 3 demonstrate that serrated flow in Pd–40Ni–20P occurs only at low strain rates and is suppressed above a critical strain rate. This observation is consistent with the recent report of Mukai *et al.,*[1] who found a marked change in the tensile fracture behavior of Pd–40Ni–20P as the strain rate was increased from $10^{-3}$ to $10^{3}$/s. At low strain rates, failure occurred along a single shear band, whereas many intersecting bands were involved in fracture at high strain rates. Since load serrations are associated with the operation of individual shear bands, this strain rate dependence of tensile fracture behavior indirectly suggests a transition from serrated to nonserrated flow at high strain rates, as observed here in Fig. 3.

The suppression of load serrations at high strain rates (Fig. 3) is also consistent with numerous observations of Kimura and Masumoto on a Pd–6Cu–16Si metallic glass.[4,10–13] In a series of experiments in mode-I or mode-III straining around a crack, these authors found that load serrations decreased in magnitude as the displacement rate increased and disappeared altogether above a critical displacement rate. The same result was found in uniaxial compression, where Kimura and Masumoto identified the critical strain rate of approximately $4 \times 10^{-3}$–$2 \times 10^{-2}$/s, above which serrated flow did not occur. Although this range of strain rates is about 2 orders of magnitude lower than the critical rate found in this work (approximately $10^{-1}$–1/s), the compositions of the Pd-based alloys used in these two studies were significantly different (Pd–6Cu–13Si in Refs. 4 and 10–13, compared with Pd–40Ni–20P in this work). The similar trends observed in Refs. 4 and 10–13 and this work therefore suggest that the transition from serrated to nonserrated flow may be common to BMGs of various compositions.

In summary, instrumented nanoindentation has been used to probe the serrated flow behavior of a Pd–40Ni–20P bulk metallic glass, where pop-in events are associated with the operation of individual shear bands. By testing over a broad range of indentation strain rates, we find that serrated flow is increasingly pronounced at lower strain rates and is suppressed at high strain rates. The trend observed here through nanoindentation measurements compares well with trends measured in various other modes of mechanical loading.

## ACKNOWLEDGMENT

This work was performed under the auspices of the United States Department of Energy at the University of California Lawrence Livermore National Laboratory, under Contract W-7405-Eng-48.

## REFERENCES


1. T. Mukai, T.G. Nieh, Y. Kawamura, A. Inoue, and K. Higashi, Scr. Mater. **46,** 43 (2002).
2. W.J. Wright, R. Saha, and W.D. Nix, Mater. Trans. Jpn. Inst. Mater. **42,** 642 (2001).
3. W.J. Wright, R.B. Schwarz, and W.D. Nix, Mater. Sci. Eng. A **319–321,** 229 (2001).
4. H. Kimura and T. Masumoto, Acta Metall. **31,** 231 (1983).
5. C.A. Pampillo and H.S. Chen, Mater. Sci. Eng. **13,** 181 (1974).
6. P.E. Donovan, Acta Metall. **37,** 445 (1989).
7. F. Szuecs, C.P. Kim, and W.L. Johnson, Acta Mater. **49,** 1507 (2001).
8. C.C. Hays, C.P. Kim, and W.L. Johnson, Phys. Rev. Lett. **84,** 2901 (2000).
9. E. Pekarskaya, C.P. Kim, and W.L. Johnson, J. Mater. Res. **16,** 2513 (2001).
10. H. Kimura and T. Masumoto, Acta Metall. **28,** 1663 (1980).
11. H. Kimura and T. Masumoto, Acta Metall. **28,** 1677 (1980).
12. H. Kimura and T. Masumoto, Philos. Mag. **44A,** 1005 (1981).
13. H. Kimura and T. Masumoto, Philos. Mag. **44A,** 1021 (1981).
14. Y.I. Golovin, V.I. Ivolgin, V.A. Khonik, K. Kitagawa, and A.I. Tyurin, Scr. Mater. **45,** 947 (2001).
15. R. Vaidyanathan, M. Dao, G. Ravichandran, and S. Suresh, Acta Mater. **49,** 3781 (2001).
16. H. Kato, Y. Kawamura, A. Inoue, and H-S. Chen, Mater. Sci. Eng. A **304–306,** 758 (2001).
17. S. Suresh, T-G. Nieh, and B.W. Choi, Scr. Mater. **41,** 951 (1999).
18. M. Pang and D.F. Bahr, J. Mater. Res. **16,** 2634 (2001).
19. S.G. Corcoran, R.J. Colton, E.T. Lilleodden, and W.W. Gerberich, Phys. Rev. **B55,** R16057 (1997).
20. A. Gouldstone, K.J. Van-Vliet, and S. Suresh, Nature **411,** 656 (2001).
21. D.F. Bahr, D.E. Kramer, and W.W. Gerberich, Acta Mater. **46,** 3605 (1998).
22. W.H. Poisl, W.C. Oliver, and B.D. Fabes, J. Mater. Res. **8,** 2024 (1995).
23. N.I. Tymiak, D.E. Kramer, D.F. Bahr, T.J. Wyrobek, and W.W. Gerberich, Acta Mater. **49,** 1021 (2001).